EFFECT OF H- AND O-TERMINATION OF NANOCRYSTALLINE DIAMOND FILMS ON CELL ADHESION AND OSTEOGENIC DIFFERENTIATION

Jana LISKOVA[a], Oleg BABCHENKO[b], Marian VARGA[b], Alexander KROMKA[b], Daniel HADRABA[a], Zdenek SVINDRYCH[a] and Lucie BACAKOVA[a]

a, Institute of Physiology, Academy of Sciences of the Czech Republic, Prague, Czech Republic, EU
b, Institute of Physics, Academy of Sciences of the Czech Republic, Prague, Czech Republic, EU
E-mail address: jana.liskova@biomed.cas.cz

Abstract

Nanocrystalline diamond (NCD) films are promising materials for tissue engineering, especially for coating bone implants. The nanostructure and morphology of NCD films can efficiently mimic the properties of natural tissues. In addition, NCD wettability can be tailored by grafting specific atoms (e.g., oxygen, hydrogen, etc.). This influences the adsorption and the final geometry of proteins, and thus the behaviour of cultivated cells. NCD films are therefore proposed as a multifunctional material for fundamental studies on the growth and adhesion of osteoblasts on bone implants, which is our particular interest.

The NCD films used in this study were grown on silicon substrates by microwave plasma-enhanced chemical vapor deposition. In order to control the hydrophobic or hydrophilic character, the NCD film surfaces were grafted by hydrogen atoms (H-termination) or by oxygen atoms (O-termination). Human mesenchymal stem cells and primary human osteoblasts were used for biological studies on H- and O-terminated NCD films. We found that cells cultivated on O-terminated NCD films exhibit better adhesion than H-terminated NCD films. In addition, the expression of osteogenic cell markers collagen and alkaline phosphatase analysed by Real-time PCR and immunostaining was higher on O-terminated films.

The higher wettability of O-terminated NCD films (contact angle 15°) is promising for the adhesion and growth of osteoblasts. An O-terminated surface also seems to promote osteogenic differentiation of the cultivated cells and the production of extracellular matrix proteins.

Keywords: Nanocrystalline Diamond Film, Osteoblast, MSC, Type I collagen, Paxillin

1. INTRODUCTION

Nano-sized diamond crystals packed in a compact form as thin films, referred to as nanocrystalline diamond films (NCD), display a wide range of unique physical and chemical properties, such as mechanical hardness, chemical and thermal resistance, excellent optical transparency and controllable electrical properties [1]. The nanostructure and morphology of NCD films can efficiently mimic the properties of natural tissues [2, 3], and so they should support cell adhesion, proliferation and differentiation. In addition, NCD wettability can be tailored by grafting specific atoms and functional chemical groups (e.g., oxygen, hydrogen, amine groups, etc.), which influence the wettability and the surface energy of NCD films [4]. NCD films are therefore proposed as multifunctional materials for fundamental studies on the growth and adhesion of osteoblasts on bone implants.

The desired integration of bone implants is dependent on the osteoconductivity of the implant surface. Osteoconduction means that the bone tissue grows on a surface or down into the pores or channels of the material [5]. Osteoconduction is achieved by the adhesion, growth and maturation of osteoblasts, manifested by the deposition of newly-formed mineralized extracellular matrix (ECM) at the bone-implant interface. The major component of organic ECM in bone tissue is type I collagen. Its fibrous structure ensures appropriate mechanical properties of the bone, which are further enhanced by matrix mineralization [6].

In this study, we have evaluated the adhesion, spreading and type I collagen production in primary human osteoblasts (pHOB) on NCD films with high or low wettability. Osteogenic differentiation of human mesenchymal stem cells (MSC) has also been analyzed on these surfaces.

2. EXPERIMENTAL

2.1 Diamond growth and surface treatment

Diamond films were deposited on p-type silicon substrates (10×10 mm2) by a microwave CVD system with an ellipsoidal cavity resonator (Aixtron P6) [7]. Before deposition, the Si substrates were ultrasonically treated in a suspension of deionised water and ultradispersed detonation diamond powder (5-10 nm in diameter). Diamond deposition was done from a gas mixture of methane and hydrogen (hydrogen gas flow of 300 sccm, methane gas flow of 3 sccm) at a total gas pressure of 5 kPa, microwave power of 2.5 kW, and a substrate temperature of around 900°C for 3 hours. The silicon substrates were coated with a diamond film from both sides (a mirror-polished side and a rough side) to minimize any unwanted interaction or effect of the Si substrate on cell cultivation. After deposition, the samples were cleaned in acids (H_2SO_4 + KNO_3) at 230°C for 30 min to reduce the non-diamond contamination [8]. Finally, one half of the prepared samples were oxidized in an RF oxygen plasma reactor for 60 seconds at 200 W, and the other half were hydrogenated in a pulsed linear antenna microwave chemical vapor deposition system for 30 minutes and at a temperature of 450°C.

2.2 Characterization of the samples

The deposited diamond films were determined from the Raman spectra acquired by a Renishaw InVia Reflex Raman spectrometer with an excitation wavelength of 442 nm. The surface morphology was investigated by scanning electron microscopy (SEM, e_LiNe workstation, Raith) in a standard configuration. The topography of the diamond films was investigated by atomic force microscopy (AFM, Solver PRO NT-MDT, Ntegra) in a tapping mode (Multi75Al-G tip). We determined the surface free energy of the samples by contact angle (CA) measurements at room temperature using a static method in a material-water droplet system [9]. Three microliters of deionized water were dropped on the plasma-treated samples and were captured by a digital CCD camera. The CA was calculated by multipoint fitting of the drop profile, using Surface Energy Evaluation software. The deposited diamond film thicknesses were evaluated from optical reflectance measurements [10].

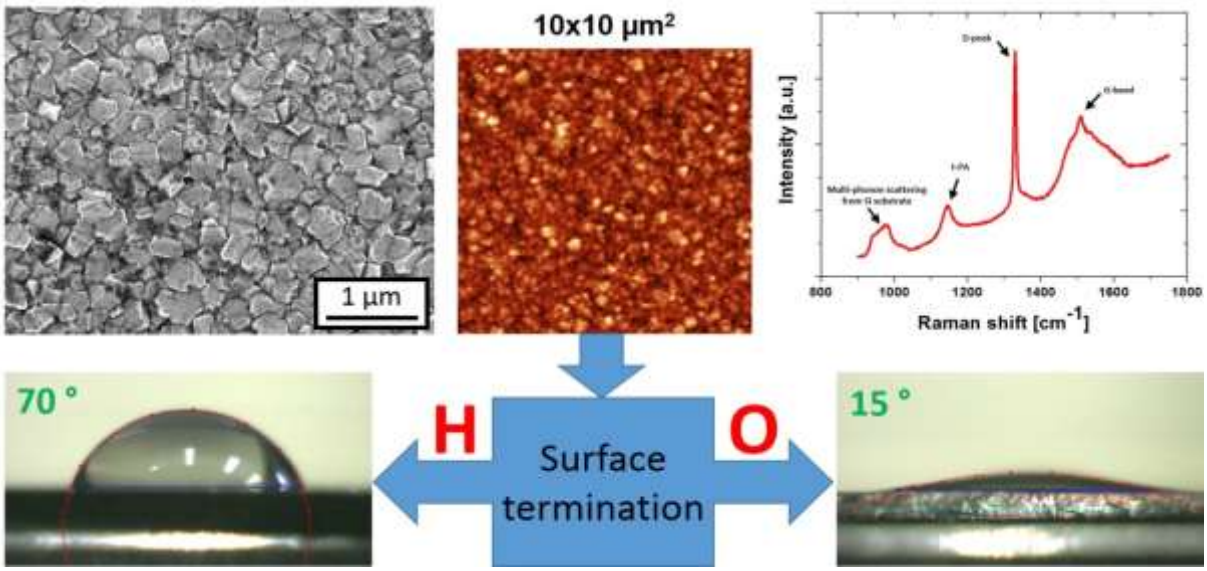

Fig. 1 SEM image, AFM image and Raman spectrum of the diamond film (top row), and wetting properties of the H-terminated and O-terminated diamond surface (bottom row).

2.3 Materials and cell culture

Square samples 1 cm^2 in size were sterilized with 70% ethanol for 1 h and washed 3 times with a sterile phosphate-buffered saline (PBS) solution. The samples were placed in 24-well polystyrene multidishes and seeded with pHOB (10000 per cm^2; 4th passage; PromoCell) or MSC (10000 per cm^2; 3rd passage; ScienCell Research Laboratories). For paxillin staining, primary human osteoblast (pHOB) cells were cultivated in a growth medium for 7 days. For type I collagen staining, pHOB cells were cultivated in a growth medium (i.e., supplemented with fetal bovine serum, FBS) for 3 days. Thereafter, the medium was supplemented with ascorbic acid (50 µg/ml), and the cells were cultivated for 1 week. Human mesenchymal stem cells (MSC) were cultivated in the growth medium for 3 days. Thereafter the medium was supplemented with ascorbic acid (50 µg/ml) and dexamethasone (10^{-7} M) and the cells were cultivated for 2 weeks. The medium was changed every 3rd day.

2.4 Immunofluorescence staining

The cells were rinsed with PBS, fixed with 70% cold ethanol and blocked with 1% bovine serum albumin in PBS (20 min). The primary antibody (dilution 1:200 in PBS) was applied overnight at 4°C. After rinsing with PBS, the cells were incubated with the secondary antibody (dilution 1:400 in PBS) for 1 hour at room temperature. The cells were then rinsed with PBS and stained with Phalloidin/Texas Red (dilution 1 µg/ml in PBS) and Hoechst 33342 (dilution 5 µg/ml) for 1 hour at room temperature. The stained cells were then rinsed with PBS and visualized and photographed under an IX 51 epifluorescence microscope equipped with a DP 70 digital camera (both manufactured by Olympus, Japan). The images were analysed using ImageJ (U. S. National Institutes of Health).

2.5 Real-time polymerase chain reaction (PCR)

On day 14, the total RNA was extracted from the cell layers with RNAzol (Molecular Research Center), according to the manufacturer's protocol. Reverse transcription was performed using oligo-dT primers with the ProtoScript M-MuLV First Strand cDNA Synthesis Kit (New England Biolabs), according to the manufacturer's protocol. The Real-time PCR reactions were performed using FastStart Universal SYBR Green Master Mix (Roche) on the iQ5 Multicolor Real-Time PCR Detection System (BioRad). The Real-time PCR parameters were: 40 cycles, 95°C for 10 s and 60°C for 1 min; the reactions were carried out in duplicate. The Real-time PCR data were analyzed in BioRad iQ software and CFX Manager software using the $\Delta\Delta C_T$ method, including the efficiencies of particular primer pairs (Tab. 1), in order to increase the accuracy of the results. The expression levels of osteoblast marker genes were normalized to the expression of the GAPDH gene, and were related to the expression levels of the cells on a polystyrene dish harvested on day 1 after seeding. The experiments were performed in duplicate and were repeated twice. The statistical analysis was performed on $\Delta\Delta C_T$ values.

2.6 Statistics

The statistical analyses were performed using SigmaStat (Jandel Corporation, San Jose, CA USA). Multiple comparison procedures were carried out by ANOVA. The pairwise multiple comparisons were counted by the Student–Newman–Keuls method. A value of $p \leq 0.05$ was considered significant.

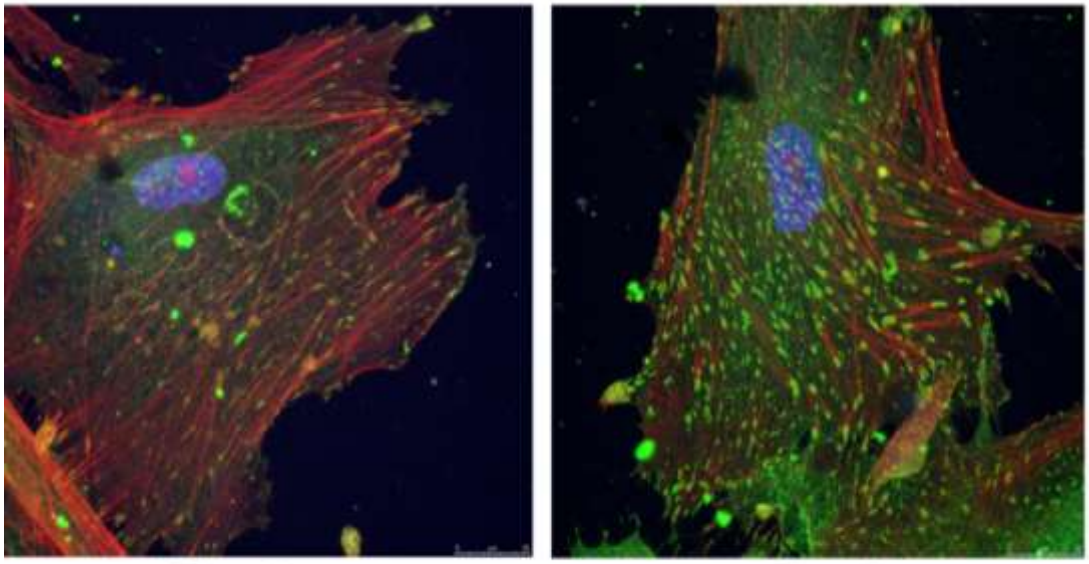

Fig. 2. pHOB cells on H-terminated (Diam. H) and O-terminated (Diam. O) NCD films, day 7. Green – paxillin, red – actin, blue – nucleus.

Table 1. Real-time PCR primers used in the study.

Gene	Primer sequences (5'-3')	Product length (bp)	Efficiency
Type I collagen	CAGCCGCTTCACCTACAGC TTTTGTATTCAATCACTGTCTTGCC	83	92.5%
ALP	GACCCTTGACCCCACAAT GCTGCTACTGCATGTCCCCT	68	90.7%
Osteocalcin	GAAGCCCAGCGGTGCA CACTACCTCGCTGCCCTCC	70	104%
GAPDH	TGCACCACCAACTGCTTAGC GGCATGGACTGTGGTCATGAG	87	93.3%

3. RESULTS AND DISCUSSION

A top view SEM image, an AFM image and the Raman spectrum of the deposited diamond film are shown in Fig. 1. All the measurements confirm a typical polycrystalline diamond film character. The estimated size of the individual grains is up to 350 nm, and the film thickness is around 420 nm. The root mean square (RMS) roughness was evaluated as 30 nm. In the Raman spectrum of the diamond film there are three characteristic features: the peak located at 1 332 cm^{-1} (diamond peak), the G-band at 1 530 cm^{-1} (sp^2 graphitic phases), and a negligible band localized at approximately 1 150 cm^{-1}, which is often assigned to transpolyacetylene (t-PA) fragments. The broad band at 950 cm^{-1} corresponds to multi-phonon scattering coming from the Si substrate [11]. The water contact angle measurements shown in the bottom row confirm hydrophobic properties with a contact angle of about 70° for the hydrogenated surface and hydrophilic properties (contact angle of 15°) for the oxidized surface.

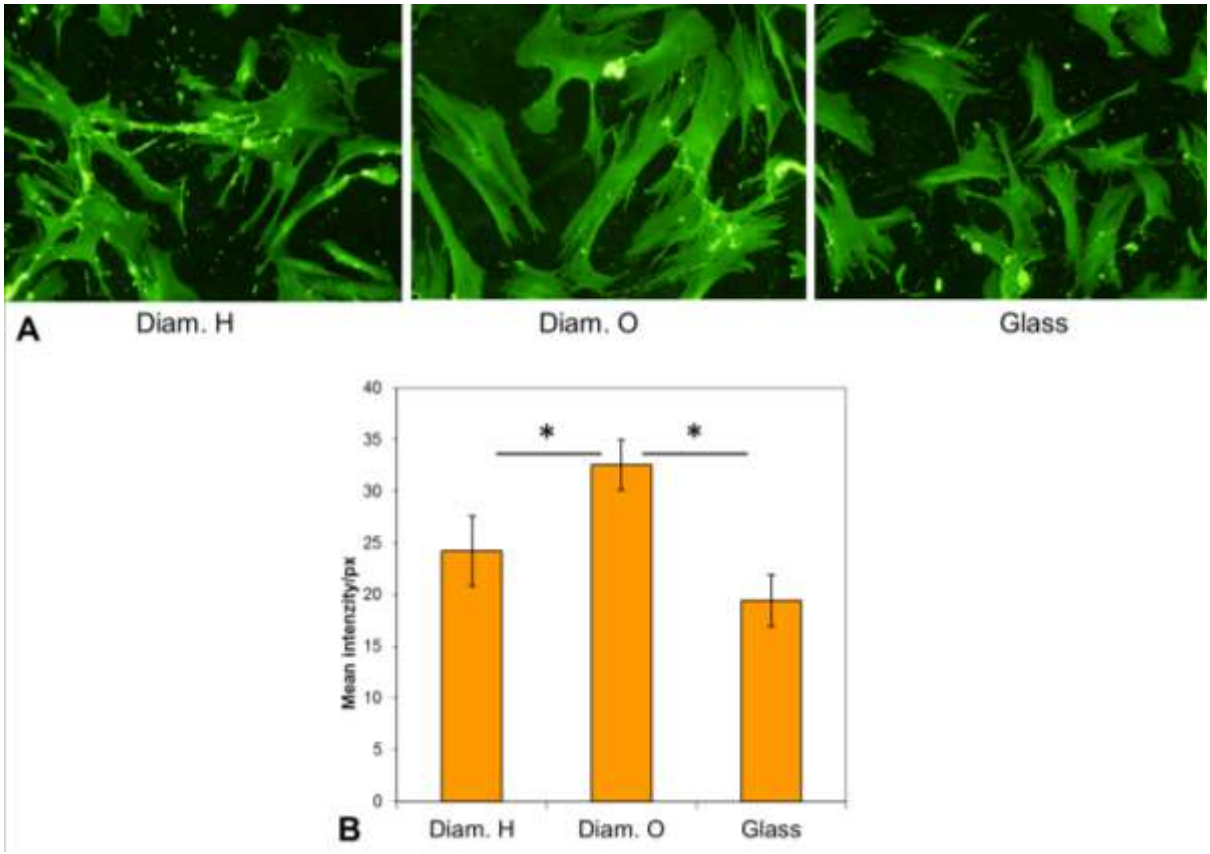

Fig. 3. pHOB cells on H-terminated (Diam. H) and O-terminated NCD films (Diam. O) and on the microscopic glass control, day 7. (A) Immunofluorescence staining of type I collagen. (B) Image analysis results for type I collagen immunofluorescence staining. The graph shows the mean of the relative fluorescence intensity per pixel.

Primary human osteoblasts (pHOB) were cultivated on NCD samples for 7 days. For the analysis of cell adhesion and spreading, the actin cytoskeleton and focal adhesion protein paxillin were stained (Fig. 2). Focal adhesions, depicted by paxillin staining, were prominent on the O-terminated NCD films but were weakly stained on the H-terminated NCD films. An actin cytoskeleton was well developed on both NCD termination variants.

The differences in cell adhesion on the H-terminated and O-terminated NCD films can be explained by different adsorption of the cell adhesion-influencing molecules from the serum of the culture medium; among others albumin, vitronectin and fibronectin. Their adsorption is influenced by the physical and chemical properties of the material surface, including the surface wettability (for a review, see [12]). A study of the adsorption of protein to surfaces with different wettability showed stronger affinity of albumin to a hydrophobic surface [13]. In addition, albumin is considered to be non-adhesive for cells [14]. The conformation of albumin and fibrinogen adsorbed to the surface was less organized when adsorbed on a hydrophobic surface than on a hydrophilic surface [13]. The secondary structure of proteins adsorbed to the surface affects the adhesion and subsequent proliferation of the cells on the surface [12]. The selectivity of the adsorption of various proteins to surfaces with different wettability may result in a different composition of the protein layer adsorbed from FBS during seeding of the cells, and this influences cell adhesion to the material [12].

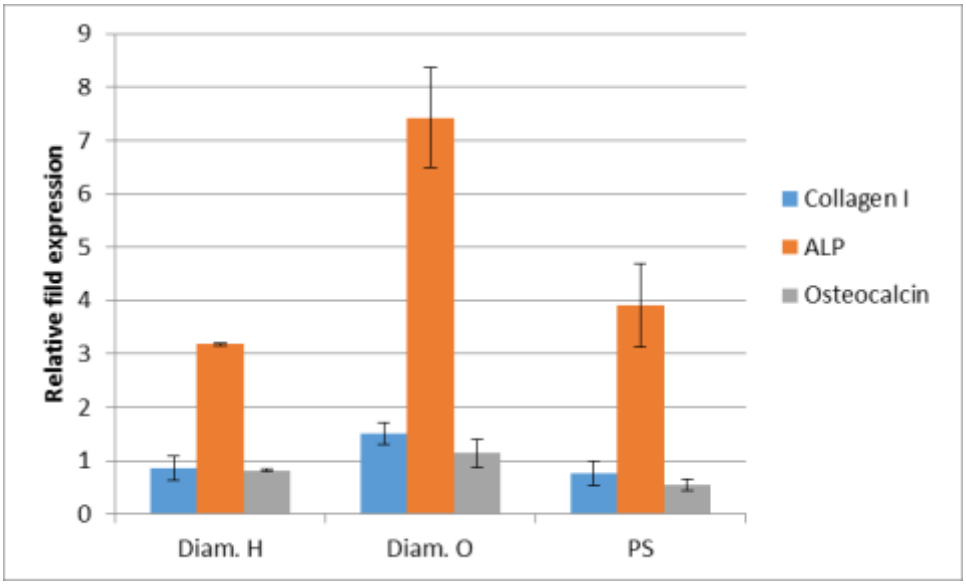

Fig. 4. Expression of marker genes of osteogenic differentiation (Type I collagen, ALP, Osteocalcin). MSCs on H-terminated (Diam. H) and O-terminated (Diam. O) NCD films and the polystyrene control (PS), day 14 of differentiation.

Type I collagen protein production was analyzed in pHOB cells growing on NCD samples by immunofluorescence staining. pHOBs were left to attach to samples for 3 days and then the cultivation medium was supplemented with ascorbic acid to support type I collagen production. After 7 days, the cells were immuno-stained and photographed. The amount of collagen protein was quantified by image analysis as relative fluorescence intensity per pixel. Figure 3 shows examples of type I collagen staining (Fig. 3 A) and fluorescence intensity quantification (Fig. 3 B). The cells exhibited a normal spread morphology, and the type I collagen protein was distributed throughout the cytoplasm of all the cells. The relative fluorescence intensity of the type I collagen staining was significantly higher ($p \leq 0.05$) on O-terminated NCD films than on H-terminated NCD films or on the control microscopic glass.

The expression of osteoblast differentiation marker genes (type I collagen, ALP and osteocalcin) was determined by reverse transcription and Real-time PCR on day 14 of cultivation of MSCs in the growth medium supplemented with osteogenic differentiation factors (Fig. 4). The expression of ALP on the O-terminated NCD films was approx. 7 fold but only approx. 3 fold on the H-terminated NCD films. The expression of type I collagen and osteocalcin remained low (0.5 – 1.5 fold). However, the type I collagen expression was higher on the O-terminated NCD films (1.511 fold) than on the N-terminated NCD films of the polystyrene control (0.858 fold, 0.761 fold; respectively).

ALP enzyme bound in cytoplasmic membrane plays an important role in bone calcification; it provides the increased phosphate concentration for hydroxyapatite crystallization [15]. Type I collagen is the major bone protein, and together with ALP they are considered as early markers of osteoblast differentiation [16]. Some other studies regard type I collagen as an early marker and ALP as a middle marker of osteogenesis [17]. Osteocalcin (also known as bone gamma-carboxyglutamic acid-containing protein; BGLAP) is a non-collagenous calcium-binding bone protein referred to as a late osteogenic marker [16].

CONCLUSION

Hydrophilic O-terminated NCD films enhance the adhesion of pHOB cells, manifested by stronger focal adhesion staining, and higher production of typical bone protein type I collagen. The expression of osteogenic marker genes in MSC cultivated on O-terminated surfaces was higher (early osteogenic markers ALP, collagen I) or similar (late osteogenic marker osteocalcin) than for cells on H-terminated surfaces.

ACKNOWLEDGEMENTS

This work has been supported within the Centre of Biomedical Research (project No. CZ.1.07/2.3.00/30.0025). This project is co-funded by the European Social Fund and by the state budget of the Czech Republic. Further support has been provided by the Grant Agency of the Czech Republic (grant No. 14-04790S), and by BIOCEV (the Biotechnology and Biomedicine Centre of the Academy of Sciences and Charles University, project No. CZ.1.05/1.1.00/02.0109), from the European Regional Development Fund.

REFERENCES

[1] BACAKOVA, L., et al., *Carbon nanoparticles as substrates for cell adhesion and growth.* Nanoparticles: New Research, 2008: p. 39-107.
[2] WEBSTER, T.J., et al., *Enhanced functions of osteoblasts on nanophase ceramics.* Biomaterials, 2000. **21**(17): p. 1803-10.
[3] WEBSTER, T.J., E.L. HELLENMEYER, and R.L. PRICE, *Increased osteoblast functions on theta + delta nanofiber alumina.* Biomaterials, 2005. **26**(9): p. 953-60.
[4] MCMAHON, R.E., et al., *Development of nanomaterials for bone repair and regeneration.* J Biomed Mater Res B Appl Biomater, 2013. **101**(2): p. 387-97.
[5] ALBREKTSSON, T. and C. JOHANSSON, *Osteoinduction, osteoconduction and osseointegration.* Eur Spine J, 2001. **10 Suppl 2**: p. S96-101.
[6] TYE, C.E., G.K. HUNTER, and H.A. GOLDBERG, *Identification of the type I collagen-binding domain of bone sialoprotein and characterization of the mechanism of interaction.* J Biol Chem, 2005. **280**(14): p. 13487-92.
[7] PRAJZLER, V., et al., *Design and investigation of properties of nanocrystalline diamond optical planar waveguides.* Optics Express, 2013. **21**(7): p. 8417-8425.
[8] VARGA, M., et al., *Optical study of defects in nano-diamond films grown in linear antenna microwave plasma CVD from H2/CH4/CO2 gas mixture.* Physica Status Solidi B-Basic Solid State Physics, 2012. **249**(12): p. 2635-2639.
[9] VARGA, M., et al., *HFCVD growth of various carbon nanostructures on SWCNT paper controlled by surface treatment.* physica status solidi (b), 2012. **249**(12): p. 2399-2403.
[10] VARGA, M., et al., *Diamond growth on copper rods from polymer composite nanofibres.* Applied Surface Science, 2014.
[11] GALÁŘ, P., et al., *Influence of non-diamond carbon phase on recombination mechanisms of photoexcited charge carriers in microcrystalline and nanocrystalline diamond studied by time resolved photoluminescence spectroscopy.* Optical Materials Express, 2014. **4**(4): p. 624-637.
[12] BACAKOVA, L., et al., *Modulation of cell adhesion, proliferation and differentiation on materials designed for body implants.* Biotechnol Adv, 2011. **29**(6): p. 739-67.
[13] ROACH, P., D. FARRAR, and C.C. PERRY, *Interpretation of protein adsorption: surface-induced conformational changes.* J Am Chem Soc, 2005. **127**(22): p. 8168-73.
[14] WANG, D.A., et al., *In situ immobilization of proteins and RGD peptide on polyurethane surfaces via poly(ethylene oxide) coupling polymers for human endothelial cell growth.* Biomacromolecules, 2002. **3**(6): p. 1286-95.
[15] ANDERSON, H.C., *Mechanism of mineral formation in bone.* Lab Invest, 1989. **60**(3): p. 320-30.
[16] ZUR NIEDEN, N.I., G. KEMPKA, and H.J. AHR, *In vitro differentiation of embryonic stem cells into mineralized osteoblasts.* Differentiation, 2003. **71**(1): p. 18-27.
[17] GONG, Z. and F.H. WEZEMAN, *Inhibitory effect of alcohol on osteogenic differentiation in human bone marrow-derived mesenchymal stem cells.* Alcohol Clin Exp Res, 2004. **28**(3): p. 468-79.